Paramagnetic Ultrasmall Gadolinium Oxide Nanoparticles as Advanced T_1 MRI Contrast Agent: Account for Large Longitudinal Relaxivity, Optimal Particle Diameter, and *In Vivo* T_1 MR Images

Ja Young Park,[†] Myung Ju Baek,[‡] Eun Sook Choi,[†] Seungtae Woo,[§] Joo Hyun Kim,[§] Tae Jeong Kim,[‡,⊥] Jae Chang Jung,[∥] Kwon Seok Chae,[¶] Yongmin Chang,[‡,§,*] and Gang Ho Lee[†,‡,*]

[†]Department of Chemistry, College of Natural Sciences, [‡]Department of Nanoscience and Nanotechnology, [§]Department of Diagnostic Radiology, School of Medicine, [⊥]Department of Applied Chemistry, College of Engineering, [∥]Department of Biology, College of Natural Sciences, and [¶]Department of Biology Education, Teachers' College, Kyungpook National University, Taegu 702-701, South Korea

ABSTRACT Paramagnetic ultrasmall gadolinium oxide (Gd_2O_3) nanoparticles with particle diameters (d) of ~1 nm were synthesized by using three kinds of Gd(III) ion precursors and by refluxing each of them in tripropylene glycol under an O_2 flow. A large longitudinal relaxivity (r_1) of water proton of 9.9 s^{-1} mM^{-1} was estimated. As a result, high contrast *in vivo* T_1 MR images of the brain tumor of a rat were observed. This large r_1 is discussed in terms of the huge surface to volume ratio (S/V) of the ultrasmall gadolinium oxide nanoparticles coupled with the cooperative induction of surface Gd(III) ions for the longitudinal relaxation of a water proton. It is found from the d dependence of r_1 that the optimal range of d for the maximal r_1, which may be used as an advanced T_1 MRI contrast agent, is 1—2.5 nm.

KEYWORDS: ultrasmall · gadolinium oxide nanoparticle · longitudinal relaxivity · T_1 MR imaging

Magnetic resonance imaging (MRI) is a very important noninvasive technique that is used to diagnose diseases.[1,2] The diagnosis of diseases through MRI is further improved by using the MRI contrast agent.[3] Two types of MRI contrast agents have been developed so far. One is the dextran coated superparamagnetic iron oxide nanoparticle, which possesses a very large transverse relaxivity (r_2) of water proton of 100−200 s^{-1} mM^{-1} (T_2 MRI contrast agent).[4−7] The other is the paramagnetic Gd(III)−chelate that possesses a longitudinal relaxivity (r_1) of water proton of 3−5 s^{-1} mM^{-1} (T_1 MRI contrast agent).[8,9] Nowadays, the latter is prevailing in clinical use because it can be generally used for all organs, whereas the former is liver-specific due to its large particle diameter.[10]

Note that the Gd(III) ion itself has been known to be the best metal ion in the periodic table which can be used as a T_1 MRI contrast agent.[9] First of all, it possesses seven unpaired 4f electrons ($^8S_{7/2}$), giving a large electron magnetic moment.[11] No other metal ions possess unpaired electrons more than this. Furthermore, these electrons solely yield the S state (no angular) electron magnetic moment, and thus, the Gd(III) ion can very efficiently induce the longitudinal relaxation of a water proton.[9]

It has been recently suggested that a T_1 MRI contrast agent more advanced (*i.e.*, more sensitive) than Gd(III)−chelates needs to be developed. Gadolinium oxide nanoparticles could be one of such candidates because they can have larger r_1 values than Gd(III)−chelates, depending on their particle diameter (d). The gadolinium oxide nanoparticles have been synthesized by several ways. The reaction between $GdCl_3$ and NaOH at elevated temperatures yielded the gadolinium oxide nanoparticles with particle diameters of 2−15 nm.[12−17] The gadolinium oxide nanoparticles with an average d of ~10 nm were synthesized from the combustion of $Gd(NO_3)_3$ and amino acid glycin.[12] The gadolinium oxide nanoparticles with an average d of ~2.3 nm were synthesized by decomposing Gd(III)−acetates encapsulated in single-wall carbon nanotubes.[18] The gadolinium oxide nanoparticles were synthesized by dehydrating $Gd(OH)_3$.[19] Gadolinium nanoparticles with different compositions were also synthesized. $GdPO_4$ nanorods with d of 20−30 nm (major axis) and 6−15 nm (minor axis) were

*Address correspondence to ghlee@mail.knu.ac.kr, ychang@knu.ac.kr.

Received for review July 7, 2009 and accepted October 13, 2009.

Published online October 16, 2009. 10.1021/nn900761s CCC: $40.75

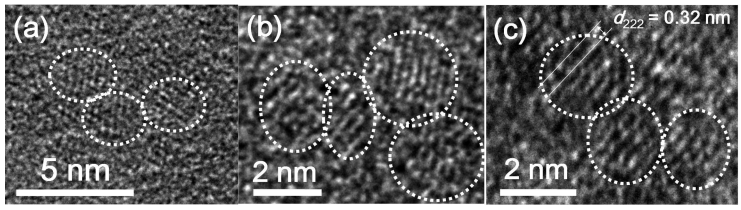

Figure 1. HRTEM micrographs of ultrasmall gadolinium oxide nanoparticles synthesized from (a) gadolinium chloride hydrate (sample A), (b) gadolinium acetate hydrate (sample B), and (c) gadolinium acetylacetonate hydrate (sample C) as Gd(III) ion precursors. Particle diameters are nearly monodisperse and estimated to be ~1 nm for samples A and C and ~1.5 nm for sample B. Provided is the lattice distance (d_{222}).

synthesized from the reaction between $Gd(NO_3)_3$ and ammonium hydrogen phosphate.[20] GdF_3 and GdF_3/LaF_3 nanoparticles with d of 10−110 nm were synthesized.[21] Most of these nanoparticles showed larger r_1 values than the Gd(III)−chelates, depending on their d.

We deal with ultrasmall gadolinium oxide nanoparticles in this work. The ultrasmall gadolinium oxide nanoparticles with an average d of 1 nm in this work provided the r_1 of 9.9 s^{-1} mM^{-1}, which is much larger than those of Gd(III)−chelates.[8,9] It seems that surface Gd(III) ions in gadolinium oxide nanoparticles cooperatively induce the longitudinal relaxation of the water proton. As a result, this cooperative induction effect accelerates the longitudinal relaxation of the water proton, providing a larger r_1 than Gd(III)−chelates. We address this by carefully examining the d dependence of r_1. We finally took *in vivo* T_1 MR images of a rat with a brain tumor by using D-glucuronic acid coated ultrasmall gadolinium oxide nanoparticles and observed a clear contrast enhancement in T_1 MR images of the tumor after injection.

RESULTS AND DISCUSSION

High-resolution transmission electron microscope (HRTEM) micrographs of ultrasmall gadolinium oxide nanoparticles synthesized from three Gd(III) ion precursors are shown in Figure 1 (also see the Supporting Information). Particle diameters are nearly monodisperse and estimated to be ~1 nm for samples synthesized from gadolinium chloride hydrate and gadolinium acetylacetonate hydrate and ~1.5 nm for a sample synthesized from gadolinium acetate hydrate. The lattice fringe of $d_{222} = 3.2 \pm 0.3$ Å in HRTEM micrographs is in agreement with that (3.13 Å) of cubic Gd_2O_3.[22] More precisely, Gd_2O_3 possesses a bixbyite structure (space group $Ia3 - T_h^7$).[23] Further details, such as the three-dimensional structure, are given by both Pauling *et al.*[23] and Moon *et al.*[24]

$M-H$ curves ($-5 \leq H \leq 5$ T) at temperatures (T) of 5 and 300 K and zero-field cooled (ZFC) $M-T$ curves ($3 \leq T \leq 330$ K) at an applied field (H) of 100 Oe were recorded (Supporting Information). Correction in magnetization was made to obtain a net magnetization of Gd(III) ions in ultrasmall gadolinium oxide nanoparticles for three samples. First, a net mass of the ultrasmall gadolinium oxide nanoparticles in each powder sample was estimated by recording a thermogravimetric analyzer (TGA) curve (Figure 2) because surfaces of the ultrasmall gadolinium oxide nanoparticles were contaminated by solvent molecules as well as moisture. Then, a net mass of Gd(III) ions in each powder sample was estimated by multiplying $m(Gd)/m(Gd_2O_3)$ (=0.8676) to the mass estimated above. The $M-H$ curves at $T = 5$ and 300 K show that both coercivity and remanence are zero for all three samples (*i.e.*, no hysteresis). This lack of hysteresis as well as no magnetic transition down to $T = 3$ K in the ZFC $M-T$ curves shows that the ultrasmall gadolinium oxide nanoparticles are paramagnetic down to $T = 3$ K, which is consistent with the neutron beam experiment.[25] From the $M-H$ curves at $T = 5$ K, saturation magnetizations were measured to be 234.1, 238.4, and 206.3 emu/g (average = 226.3 emu/g) at $H = 5$ T for the three samples, respectively, corresponding to 6.6, 6.7, and 5.8 μ_B per atom (average = 6.4 μ_B per atom), respectively. This average value is slightly less than 6.9 μ_B per atom of Gd_2O_3,[26] primarily because the $M-H$ curves are not completely saturated at $H = 5$ T.

In order to measure both relaxivity and *in vivo* T_1 MR images, ultrasmall gadolinium oxide nanoparticles were coated by hydrophilic and biocompatible D-glucuronic acid because of the toxicity of the Gd(III) ion. The coating was characterized by recording both a Fourier transform infrared (FT-IR) absorption spectrum and a TGA curve of a powder sample (Figure 3a,b, respectively). The observed absorption frequencies characteristic of the D-glucuronic acid in D-glucuronic acid coated ultrasmall gadolinium oxide nanoparticles include the C−H stretch at ~2910 cm^{-1}, the C═O stretch at ~1610 cm^{-1}, and the C−O stretch at ~1080 cm^{-1}. It is known that a carboxylic acid chemically binds to surface metal ions.[12,27−30] This can be noticed from the red-shifted C═O stretch. In the present case, the C═O stretch is red-shifted by ~100 cm^{-1} from ~1710 cm^{-1} of the free D-glucuronic acid, which is consistent with gadolinium oxide nanoparticles coated by various carboxylic acids.[12] The TGA curve shows enough surface

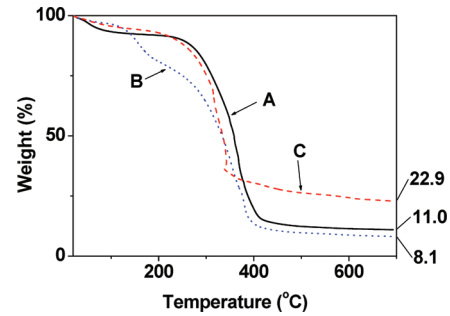

Figure 2. TGA curves of ultrasmall gadolinium oxide nanoparticles (*i.e.*, samples A, B, and C in Figure 1). The net weight percentages of the remaining gadolinium oxide nanoparticles after TGA experiment are provided on the right.

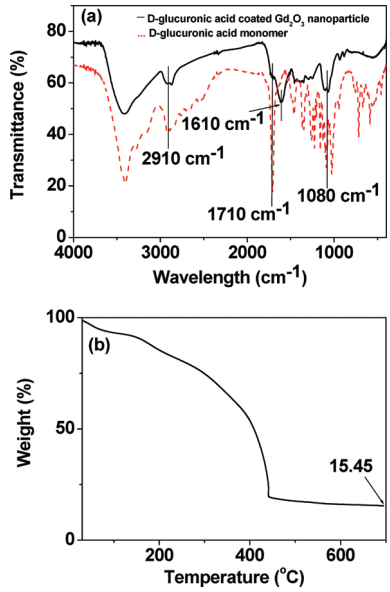

Figure 3. (a) FT-IR spectrum and (b) TGA curve of D-glucuronic acid coated ultrasmall gadolinium oxide nanoparticles. FT-IR absorption spectrum of D-glucuronic acid is provided as a reference.

coating of the ultrasmall gadolinium oxide nanoparticles by the D-glucuronic acid (*i.e.*, with maximum coating of 84.55% because of remaining some moisture and solvent).

The longitudinal (T_1) and transverse (T_2) relaxation times were measured at various solutions of different Gd(III) ion concentrations. The r_1 and r_2 were then estimated to be 9.9 and 10.5 s^{-1} mM^{-1} from the slopes of the $1/T_1$ ($=R_1$) and $1/T_2$ ($=R_2$) plots *versus* Gd(III) ion concentration, respectively (Figure 4a). The r_2/r_1 ratio is estimated to be 1.06. The R_1 and R_2 map images were also measured (Figure 4b,c, respectively). They show a clear dose-dependent color change which is due to the relaxation increase of the water proton with increasing the dose. This suggests a high sensitivity of ultrasmall gadolinium oxide nanoparticles as T_1 MRI contrast agent. In general, the r_1 should be as large as possible, and the r_2/r_1 ratio should be as close to 1 as possible in order for a chemical to be used as a highly sensitive T_1 MRI contrast agent. The ultrasmall gadolinium oxide nanoparticles seem to satisfy both conditions to a great extent.

Our r_1 and those of others are provided in Table 1 and are also plotted as a function of d in Figure 5a. In this plot, $Gd(TETA)^-$ was assumed to be the smallest nanoparticle with d of 0.1 nm. The plot clearly shows that the r_1 depends on d. Assuming Gaussian, Lorentzian, and log-normal functions for the dependence, the maximal r_{1max} and d_{max} were estimated from the corresponding function fits (Figure 5b) and are provided in Table 2. These fits suggest that the optimal range of d for the maximal r_1 will be 1−2.5 nm. Therefore, the gadolinium oxide nanoparticles with d in this range may be used as an advanced T_1 MRI contrast agent.

This dependence of r_1 on d can be reproduced by considering two factors which include one increasing and the other decreasing factors of r_1 with d. First, the decreasing factor may be considered as the surface to volume ratio (S/V) because the r_1 drops to a negligible value as d approaches the bulk, as shown in Figure 5a as well as in Table 1. This indicates that only the surface Gd(III) ions significantly contribute to the longitudinal relaxation of the water proton. We may simply write this dependence as $r_1 \propto S/V$. By using an approximate formula $S/V \approx 4(a/d)$ in which a is the average diameter of Gd(III) and O^{2-} ions (0.234 nm)[31] and $d \sim 1$ nm observed in this work; the S/V of ultrasmall gadolinium oxide nanoparticles is estimated to be 0.936, indicating that nearly all of the Gd(III) ions are surface ones and, thus, may significantly contribute to the longitudinal relaxation of the water proton. Second, the increasing factor may be constructed by realizing that the gadolinium oxide nanoparticles with d less than ~4.0 nm possess larger r_1 values than Gd(III)−chelates (see Figure 5a as well as Table 1). Because r_1 is measured in s^{-1} mM^{-1}, it could not be larger than those of Gd(III)−chelates. Two kinds of theories for the longitudinal relaxation of the water proton exist.[8] One is the inner-sphere model applied to water molecules directly coordinated to Gd(III) ion as in $Gd(DTPA)(H_2O)^{2-}$ in Table 1. The other is the outer-sphere model applied to water molecules around the fully coordinated Gd(III) ion as in $Gd(TETA)^-$ in Table 1. For the surface coated gado-

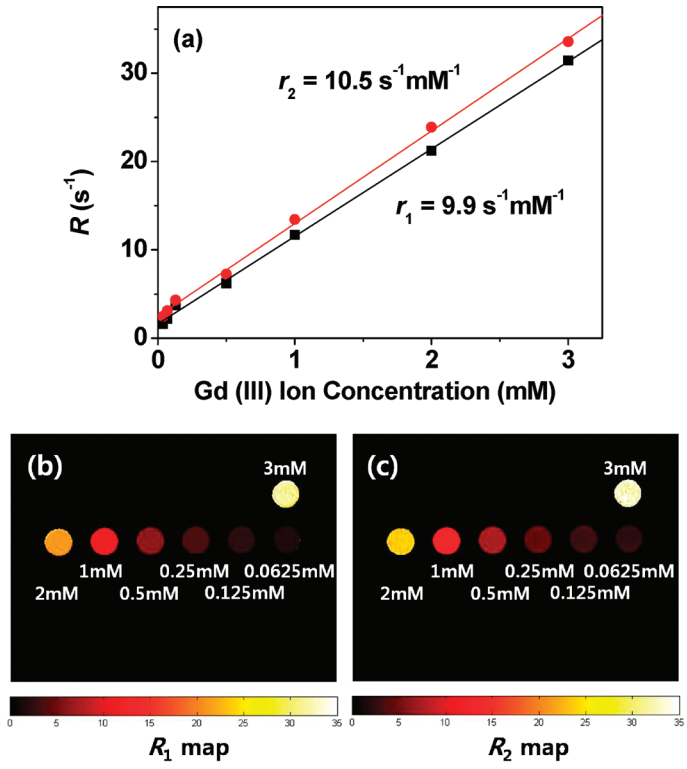

Figure 4. (a) Plots of the R_1 and R_2 as a function of Gd(III) ion concentration. Slopes provide the r_1 and r_2. (b) R_1 and (c) R_2 map images as a function of Gd(III) ion concentration.

TABLE 1. Relaxivity (r_1) of Ligand Coated Gadolinium Oxide Nanoparticles and Gd(III)−Chelates (the ligand used and the average particle diameter (d_{avg}) are provided)

chemical	ligand	d_{avg} (nm)	r_1 (s^{-1} mM^{-1})	r_2/r_1	reference
Gd(III)−H_2O[a]	DTPA[c]		4.1	1.1	8
Gd(III)[b]	TETA[d]		2.1		8
Gd_2O_3	D-glucuronic acid	1.0	9.9	1.1	this work
Gd_2O_3	PEG−silane	2.2	8.8	1.3	17
Gd_2O_3	PEG−silane	3.8	8.8	3.4	17
Gd_2O_3	PEG−silane	4.6	4.4	6.8	17
Gd_2O_3	PEG−silane	30	0.1	81.6	14

[a]One water added. [b]No water is directly coordinated to Gd(III) ion. [c]Diethylenetriaminepentaacetic acid. [d]1,4,8,11-Tetraazacyclotetradecane-*N*,*N*′,*N*′′,*N*′′′-tetraacetic acid.

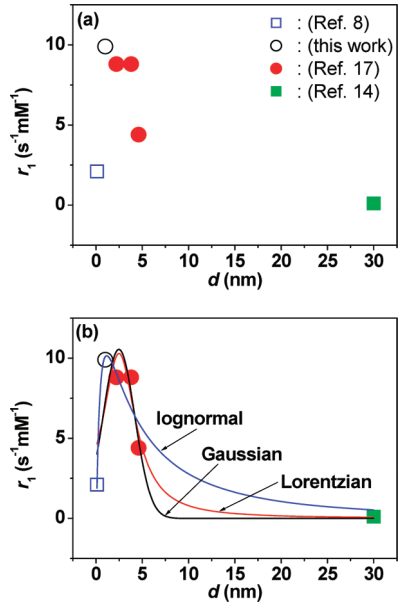

Figure 5. (a) Plot of r_1 as a function of d and (b) three kinds of function fits to the plot. Gd(TETA)$^-$ was used as the smallest nanoparticle with d of 0.1 nm.

linium oxide nanoparticles, the outer-sphere model will be applied because the ultrasmall gadolinium oxide nanoparticles are heavily coated by D-glucuronic acid, as can be noticed from the TGA curve (Figure 3b). One possibility for the increasing factor is that several surface Gd(III) ions cooperatively induce the longitudinal relaxation of the water proton and, as a result, accelerate it. This is schematically shown in Figure 6a, where four surface Gd(III) ions as an example participate in this cooperative induction. However, individual Gd(III) ions in molecular Gd(III)−chelates cannot afford this because they are separated far apart (Figure 6b). We may simply write this dependence as $r_1 \propto$ the number (N) of cooperative surface Gd(III) ions. By using 2.1 s^{-1} mM^{-1} for $N = 1$ from Gd(TETA)$^-$ and the r_{1max} values estimated from the three kinds of function fits above, the maximum numbers (N_{max}) of cooperative surface Gd(III) ions are consistently estimated to be ~5 for all function fits and are provided in Table 2. It is expected that N will range from 1 to N_{max} such that it approaches the N_{max} as d approaches the bulk. Taking into account the above two factors together, we may write that $r_1 \propto 2.1$ (increasing factor) × (decreasing factor), that is,

$$r_1 \propto 2.1N(S/V) \quad (1)$$

for gadolinium oxide nanoparticles. By using the N_{max} and d_{max} estimated from the three kinds of function fits, assuming that $N = N_{max}$ for $d \geq d_{max}$ and a linear decrease of N from N_{max} to 1 for $d < d_{max}$, and assuming that the S/V is 1 for $d < 1$ nm, r_1 values were calculated by using eq 1. After they are multiplied by proper constants to match their heights with 9.9 s^{-1} mM^{-1} of the experimental data, the height-adjusted r_1 values are plotted in Figure 7. Note that all look consistent with the experimental data. This suggests that the above two factors really account for the dependence.

Finally, we took 3 T *in vivo* T_1 MR images of a rat with a brain tumor. Before we carried out this measurement, we performed an *in vitro* cytotoxicity test of a sample solution by using two different cell lines up to 5 μM (Figure 8a). This test shows that D-glucuronic acid coated ultrasmall gadolinium oxide nanoparticles are not toxic for the tested concentration range of Gd(III) ion, although the toxicity increased a little bit as the concentration increased. A series of 3 T *in vivo* T_1 MR im-

TABLE 2. Values of d_{max} and r_{1max} Obtained from the Three Kinds of Function Fits to the Experimental r_1 As Shown in Figure 5b and the Corresponding N_{max}

	d_{max} (nm)	r_{1max} (s^{-1} mM^{-1})	N_{max}
Gaussian[a]	2.48	10.6	5
Lorentzian[a]	2.49	10.3	5
log-normal[a]	1.10	10.1	5

[a]The baseline of r_1 in all the fits was fixed to 0.

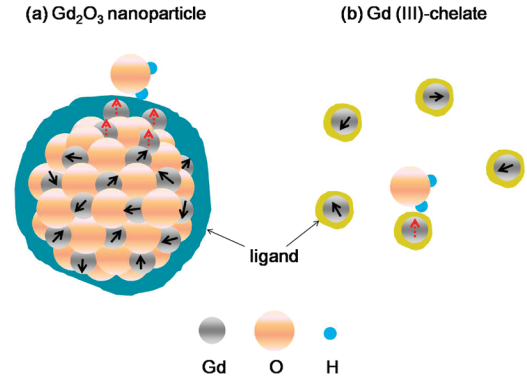

Figure 6. Schematic diagram showing that (a) four surface Gd(III) ions as an example cooperatively induce the longitudinal relaxation of the water proton, whereas (b) such an effect does not exist in individual Gd(III)−chelates. The interacting and noninteracting Gd(III) ions with a water proton are denoted as dotted and solid arrows for their spins, respectively. The ligands are drawn arbitrarily.

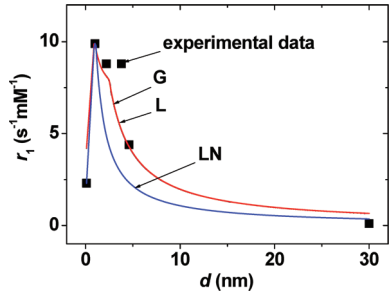

Figure 7. Reproductions of r_1 by using both eq 1 and the d_{max} and N_{max} in Table 2. They are labeled as G (Gaussian), L (Lorentzian), and LN (log-normal). The heights were adjusted to 9.9 s^{-1} mM^{-1} of the experimental data by multiplying constants to the corresponding plots (*i.e.*, 2.005 to G, 2.010 to L, and 1.095 to LN). The two plots (G and L) almost overlap with each other because their d_{max} and N_{max} values are similar to each other.

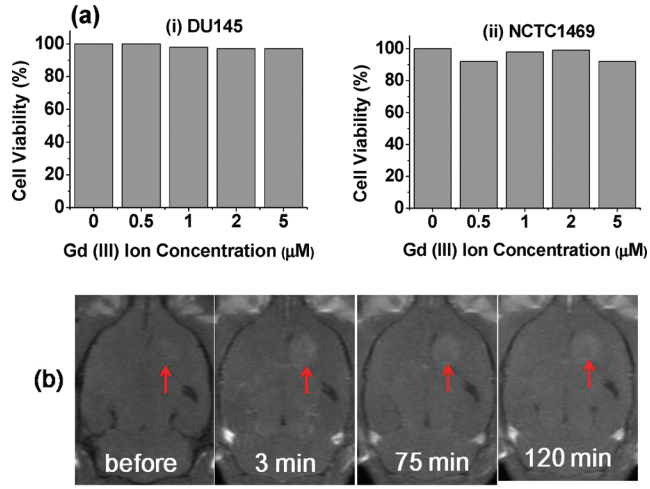

Figure 8. (a) *In vitro* cytotoxicity test of a sample solution by using (i) DU145 and (ii) NCTC1469 cell lines. (b) Series of *in vivo* T_1 MR images of a brain tumor of a rat (marked by an arrow) before and after injection of the sample solution.

ages of a rat brain are provided in Figure 8b. These T_1 MR images clearly show a high contrast enhancement of the tumor after injection. In the case of the brain tumor, the brain−blood barrier (BBB) is broken. As a result, the sample solution can easily cross the BBB, causing a contrast enhancement in the brain tumor. The contrast slightly increased as the time passed, but then slightly decreased after 120 min due to the excretion of the injected sample solution.

For clinical application, the sample solution should be excreted through kidney and bladder. Figure 9a,b shows a series of *in vivo* 3 T T_1 MR images of both kidney and bladder after vein injection of the sample solution. These MR images show a renal excretion of the sample solution. We also observed a blood pool effect of the sample solution. Figure 9c clearly shows a contrast enhancement of an aorta for a prolonged time after the vein injection. Although not quantitative, the brain tumor, kidney, bladder, and aorta MR images all together qualitatively show a wide biodistribution of the sample solution in a rat with a brain tumor. This is likely because of ultrasmall dimension of the D-glucuronic acid coated ultrasmall gadolinium oxide nanoparticles. Furthermore, it is expected that the D-glucuronic acid coated ultrasmall gadolinium oxide nanoparticle will be extremely valuable for target-

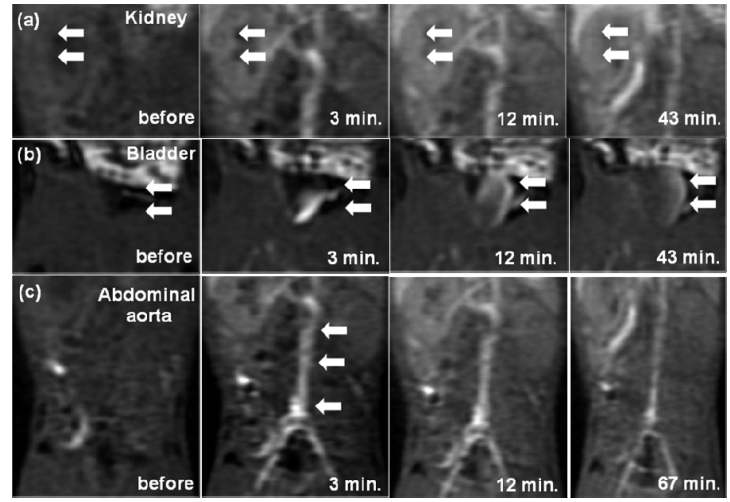

Figure 9. *In vivo* T_1 MR images of a rat with a brain tumor. (a) Kidney and (b) bladder contrast enhancement after injection of the sample solution. These MR images clearly show that the sample solution was excreted by the renal pathway. (c) In addition, the sample solution shows a blood pool effect: a long blood circulation time with a prolonged abdominal aorta contrast enhancement.

specific cancer detection, which we plan to do in the near future.

METHODS

Materials. Gadolinium chloride hydrate ($GdCl_3 \cdot xH_2O$), gadolinium acetate hydrate ($(CH_3CO_2)_3Gd \cdot xH_2O$), and gadolinium acetylacetonate hydrate ($[CH_3COCH{=}(O-)CH_3]_3Gd \cdot xH_2O$) as Gd(III) ion precursors, air as an oxygen source, tripropylene glycol as a solvent (boiling point = 273 °C), and D-glucuronic acid as a surface coating ligand were used. All chemicals except for air were purchased from Aldrich and used as received.

Synthesis of Ultrasmall Gadolinium Oxide Nanoparticles. Five millimole of a Gd(III) ion precursor was mixed with 50 mL of tripropylene glycol and magnetically stirred at 100 °C until the precursor was completely dissolved into solvent. Reaction temperature was increased to 250−260 °C and refluxed at that temperature for 24 h while air was passed through the solvent. After the reaction, the reaction solution cooled to room temperature, and the precipitate was washed with distilled water three times. For this, 400 mL of distilled water was added to the reaction solution, and the top solution was decanted after the reaction product was settled down in a few days or so. This procedure was repeated three times. A powder sample was obtained by drying the reaction product in air and then used for characterization. The same procedure was used for all three precursors.

Synthesis of D-Glucuronic Acid Coated Ultrasmall Gadolinium Oxide Nanoparticles. For both relaxivity and *in vivo* T_1 MR image measurements, ultrasmall gadolinium oxide nanoparticles were coated with hydrophilic and biocompatible D-glucuronic acid. Gadolin-

ium chloride hydrate was used as a Gd(III) ion precursor. The ultrasmall gadolinium oxide nanoparticles were first synthesized by using the same reaction procedure described above. After this, the reaction temperature was lowered to 150 °C and 5 mmol of D-glucuronic acid was added to the reaction solution. The reaction continued for 24 h at this temperature. The reaction solution cooled to room temperature. D-Glucuronic acid coated ultrasmall gadolinium oxide nanoparticles were washed with distilled water three times to remove any remaining unreacted Gd(III) ions in solution by using the same procedure described above. Powder sample was obtained by drying part of the D-glucuronic acid coated ultrasmall gadolinium oxide nanoparticles in air and was then used for characterization. The remaining part was dispersed in distilled water (total 40 mL), and then, 2 mmol of sodium citrate was added to the solution to increase the colloidal stability of the D-glucuronic acid coated ultrasmall gadolinium oxide nanoparticles in solution. However, ζ potential measurement (Supporting Information) showed that the colloidal stability only slightly increased after the sodium citrate was added. For this, the solution was heat-treated at 120 °C for 5 min (as done in dextran coated iron oxide nanoparticles)[32] and then cooled to room temperature. This solution was used as a sample solution for both relaxivity and *in vivo* T_1 MR image measurements.

Characterization. A HRTEM (JEOL, JEM 2100F, 200 kV acceleration voltages) was used to measure the *d* of ultrasmall gadolinium oxide nanoparticles. For HRTEM measurement, nanoparticles were dispersed in methanol (99.999%, Aldrich) and were then loaded onto a copper grid which was covered with an amorphous carbon membrane. A dynamic light scattering (DLS) particle size analyzer (Microtrac, UAP-150) was used to measure the hydrodynamic diameter of D-glucuronic acid coated ultrasmall gadolinium oxide nanoparticles, and it was estimated to be ~4 nm (see the Supporting Information). A superconducting quantum interference device (SQUID) magnetometer (Quantum Design, MPMS-7) was used to characterize magnetic properties of the ultrasmall gadolinium oxide nanoparticles. Both $M-H$ curves ($-5 \leq H \leq 5$ T) at $T = 5$ and 300 K and ZFC $M-T$ curves ($3 \leq T \leq 330$ K) at $H = 100$ Oe were recorded. To measure these curves, an exact mass (10−20 mg) of a powder sample was loaded into a capsule. D-Glucuronic acid coating of the ultrasmall gadolinium oxide nanoparticles was characterized with a FT-IR absorption spectrometer (Mattson Instruments, Inc., Galaxy 7020A). To record a FT-IR absorption spectrum (400−4000 cm^{-1}), a pellet was made by pressing a mixture of a powder sample and KBr. The amount of surface coating was measured with a TGA (TA Instruments, SDT Q 600). The TGA curve was scanned between room temperature and 700 °C while an air was flowed. Both the r_1 and r_2 were measured by using a MRI instrument (GE 1.5 T, Excite) equipped with the Knee coil (EXTREM). The experiment for this has been described in detail previously.[33] Gd(III) ion concentration of an original sample solution was measured with an inductively coupled plasma atomic emission spectrometer (ICPAES) (Thermo Jarrell Ash Co., IRIS/AP). Then, seven solutions of different Gd(III) ion concentrations (3, 2, 1, 0.5, 0.25, 0.125, 0.0625 mM) were prepared by diluting the original sample solution with distilled water and were used for both relaxivity and map image measurements. *In vitro* cytotoxicity test of the sample solution was performed by using the human prostate cancer cell line (DU145) and the mouse normal hepatocyte cell line (NCTC1469) for Gd(III) ion concentration up to 5 μM. Each cell viability was normalized with respect to the corresponding control cell lines with 0.0 M Gd(III) ion concentration. Three tesla *in vivo* T_1 MR images were obtained with a MRI instrument (GE 3 T, Signa HD). To obtain them, 0.07 mmol Gd/kg of the sample solution was injected into the tail vein of a rat with a brain tumor. A series of T_1 MR images of various organs such as the brain tumor, kidney, bladder, and aorta were then taken with a time interval after injection of the sample solution. The rat did not die after experiment.

Acknowledgment. This project is supported by Grant No. RTI04-01-01 from the Regional Technology Innovation Program of the Ministry of Commerce, Industry, and Energy funded by the Korean Government, by the Korea Research Foundation Grant funded by the Korean Government (KRF-2008-313-C00416), and by the Kyungpook National University Research Fund (2008). We thank the Korea Basic Science Institute for allowing us to use their HRTEM.

Supporting Information Available: HRTEM micrographs and magnetic data such as $M-H$ and $M-T$ curves for three samples, hydrodynamic diameter of D-glucuronic acid coated ultrasmall gadolinium oxide nanoparticles, and ζ potentials of D-glucuronic acid coated ultrasmall gadolinium oxide nanoparticles in distilled water, 0.05 M citrated solution, and citrated isotonic solution. This material is available free of charge *via* the Internet at http://pubs.acs.org.

REFERENCES AND NOTES

1. Hashemi, R. H.; Bradley, W. G.; Lisanti, C. J. *MRI The Basics*; Lippincott Williams & Wilkins: New York, 2004.
2. Weissleder, R.; Mahmood, U. Molecular Imaging. *Radiology* **2001**, *219*, 316−333.
3. Pankhurst, Q. A.; Connolly, J.; Jones, S. K.; Dobson, J. Applications of Magnetic Nanoparticles in Biomedicine. *J. Phys. D: Appl. Phys.* **2003**, *36*, R167–R181.
4. Jung, C. W.; Jacobs, P. Physical and Chemical Properties of Superparamagnetic Iron Oxide MR Contrast Agents: Ferumoxides, Ferumoxtran, Ferumoxsil. *Magn. Reson. Imaging* **1995**, *13*, 661–674.
5. Billotey, C.; Wilhelm, C.; Devaud, M.; Bacri, J. C.; Bittoun, J.; Gazeau, F. Cell Internalization of Anionic Maghemite Nanoparticles: Quantitative Effect on Magnetic Resonance Imaging. *Magn. Reson. Med.* **2003**, *49*, 646–654.
6. Chapon, C.; Franconi, F.; Lemaire, L.; Marescaux, L.; Legras, P.; Saint-André, J. P.; Denizot, B.; Le Jeune, J.-J. High Field Magnetic Resonance Imaging Evaluation of Superparamagnetic Iron Oxide Nanoparticles in a Permanent Rat Myocardial Infarction. *Invest. Radiol.* **2003**, *38*, 141–146.
7. Lee, J.-H.; Huh, Y.-M.; Jun, Y.-W.; Seo, J.-W.; Jang, J.-T.; Song, H.-T.; Kim, S.; Cho, E.-J.; Yoon, H.-G.; Suh, J.-S.; Cheon, J. Artificially Engineered Magnetic Nanoparticles for Ultra-Sensitive Molecular Imaging. *Nat. Med.* **2007**, *13*, 95–99.
8. Lauffer, R. B. Paramagnetic Metal Complexes as Water Proton Relaxation Agents for NMR Imaging: Theory and Design. *Chem. Rev.* **1987**, *87*, 901–927.
9. Caravan, P.; Ellison, J. J.; McMurry, T. J.; Lauffer, R. B. Gadolinium(III) Chelates as MRI Contrast Agents: Structure, Dynamics, and Applications. *Chem. Rev.* **1999**, *99*, 2293–2352.
10. Weissleder, R.; Elizondo, G.; Wittenberg, J.; Rabito, C. A.; Bengele, H. H.; Josephson, L. Ultrasmall Superparamagnetic Iron Oxide: Characterization of a New Class of Contrast Agents for MR Imaging. *Radiology* **1990**, *175*, 489–493.
11. Cotton, F. A.; Wilkinson, G. *Advanced Inorganic Chemistry*; John Wiley & Sons: New York, 1980.
12. Söderlind, F.; Pedersen, H.; Petoral, R. M.; Käll, P.-O.; Uvdal, K. Synthesis and Characterization of Gd_2O_3 Nanocrystals Functionalised by Organic Acids. *J. Colloid Interface Sci.* **2005**, *288*, 140–148.
13. Engström, M.; Klasson, A.; Pedersen, H.; Vahlberg, C.; Käll, P.-O.; Uvdal, K. High Proton Relaxivity for Gadolinium Oxide Nanoparticles. *Magn. Reson. Mater. Phys* **2006**, *19*, 180–186.
14. Fortin, M.-A.; Petoral, R. M.; Söderlind, F.; Klasson, A.; Engström, M.; Veres, T.; Käll, P.-O.; Uvdal, K. Polyethylene Glycol-Covered Ultra-Small Gd_2O_3 Nanoparticles for Positive Contrast at 1.5 T Magnetic Resonance Clinical Scanning. *Nanotechnology* **2007**, *18*, 395501.
15. Bazzi, R.; Flores, M. A.; Louis, C.; Lebbou, K.; Zhang, W.; Dujardin, C.; Roux, S.; Mercier, B.; Ledoux, G.; Bernstein, E.; Perriat, P.; Tillement, O. Synthesis and Properties of Europium-Based Phosphors on the Nanometer Scale: Eu_2O_3, Gd_2O_3:Eu, and Y_2O_3:Eu. *J. Colloid Interface Sci.* **2004**, *273*, 191–197.
16. Petoral, R. M.; Söderlind, F.; Klasson, A.; Suska, A.; Fortin, M. A.; Abrikossova, N.; Selegård, L.; Käll, P.-O.; Engström,

M.; Uvdal, K. Synthesis and Characterization of Tb^{3+}-Doped Gd_2O_3 Nanocrystals: A Bifunctional Material with Combined Labeling and MRI Contrast Agent Properties. *J. Phys. Chem. C* **2009**, *113*, 6913–6920.
17. Bridot, J.-L.; Faure, A.-C.; Laurent, S.; Rivière, C.; Billotey, C.; Hiba, B.; Janier, M.; Josserand, V.; Coll, J.-L.; Elst, L. V.; Muller, R.; Roux, S.; Perriat, P.; Tillement, O. Hybrid Gadolinium Oxide Nanoparticles: Multimodal Contrast Agents for *In Vivo* Imaging. *J. Am. Chem. Soc.* **2007**, *129*, 5076–5084.
18. Miyawaki, J.; Yudasaka, M.; Imai, H.; Yorimitsu, H.; Isobe, H.; Nakamura, E.; Lijima, S. Synthesis of Ultrafine GdO Nanoparticles inside Single-Wall Carbon Nanohorns. *J. Phys. Chem. B* **2006**, *110*, 5179–5181.
19. Chang, C.; Mao, D. Thermal Dehydration Kinetics of a Rare Earth Hydroxide, $Gd(OH)_3$. *Int. J. Chem. Kinet.* **2007**, *39*, 75–81.
20. Hifumi, H.; Yamaoka, S.; Tanimoto, A.; Citterio, D.; Suzuki, K. Gadolinium-Based Hybrid Nanoparticles as a Positive MR Contrast Agent. *J. Am. Chem. Soc.* **2006**, *128*, 15090–15091.
21. Evanics, F.; Diamente, P. R.; van Veggel, F. C. J. M.; Stanisz, G. J.; Prosser, R. S. Water-Soluble GdF_3 and GdF_3/LaF_3 Nanoparticles—Physical Characterization and NMR Relaxation Properties. *Chem. Mater.* **2006**, *18*, 2499–2505.
22. Curtis, C. E.; Johnson, J. R. Ceramic Properties of Samarium Oxide and Gadolinium Oxide: X-ray Studies of Other Rare-Earth Oxides and Some Compounds. *J. Am. Ceram. Soc.* **1957**, *40*, 15–19.
23. Pauling, L.; Shappell, M. D. The Crystal Structure of Bixbyite and the C-Modification of the Sesquioxides. *Z. Kristallogr.* **1930**, *75*, 128–142.
24. Moon, R. M.; Koehler, W. C.; Child, H. R.; Raubenheimer, L. J. Magnetic Structures of Er_2O_3 and Yb_2O_3. *Phys. Rev.* **1968**, *176*, 722–731.
25. Moon, R. M.; Koehler, W. C. Magnetic Properties of Gd_3O_3. *Phys. Rev. B* **1975**, *11*, 1609–1622.
26. Schinkel, C. J.; Van Amstel, W. D. Reduced Magnetic Moment of Gadolinium in the Oxide and the Sulphate. *Phys. Lett. A* **1973**, *44*, 467–468.
27. Mendive, C. B.; Bredow, T.; Blesa, M. A.; Bahnemann, D. W. ATR-FTIR Measurements and Quantum Chemical Calculations Concerning the Adsorption and Photoreaction of Oxalic Acid on TiO_2. *Phys. Chem. Chem. Phys.* **2006**, *8*, 3232–3247.
28. Hug, S. J.; Bahnemann, D. Infrared Spectra of Oxalate, Malonate and Succinate Adsorbed on the Aqueous Surface of Rutile, Anatase and Lepidocrocite Measured with *In Situ* ATR-FTIR. *J. Electron Spectrosc.* **2006**, *150*, 208–219.
29. Duckworth, O. W.; Martin, S. C. Surface Complexation and Dissolution of Hematite by C_1-C_6 Dicarboxylic Acids at pH = 5.0. *Geochim. Cosmochim. Acta* **2001**, *65*, 4289–4301.
30. Roddick-Lanzilotta, A. D.; McQuillan, A. J. An *In Situ* Infrared Spectroscopic Investigation of Lysine Peptide and Polylysine Adsorption to TiO_2 from Aqueous Solutions. *J. Colloid Interface Sci.* **1999**, *217*, 194–202.
31. Dean, J. A. *Lange's Handbook of Chemistry*; McGraw-Hill, Inc.: New York, 1992.
32. Groman, E. V.; Josephson, L.; Lewis, J. M. Biologically Degradable Superparamagnetic Materials for Use in Clinical Applications. U.S. Patent No. 4827945, 1989.
33. Park, J. Y.; Daksha, P.; Lee, G. H.; Woo, S.; Chang, Y. Highly Water-Dispersible PEG Surface Modified Ultra Small Superparamagnetic Iron Oxide Nanoparticles Useful for Target-Specific Biomedical Applications. *Nanotechnology* **2008**, *19*, 365603.